Full Length Research Paper

Investigation of gravity anomalies in parts of Niger Delta Region in Nigeria using aerogravity data

Ekpa M. M. M.[1], Okeke F. N.[2], Ibuot J. C.[2*], Obiora D. N.[2] and Abangwu U. J.[2]

[1]Department of Physics, School of Science Education, Federal College of Education (Technical), Omoku, Rivers State, Nigeria.
[2]Department of Physics and Astronomy, Faculty of Physical Sciences, University of Nigeria, Nsukka, Enugu State, Nigeria.

Gravity anomalies in parts of the Niger Delta region, Nigeria, were investigated through the interpretation of aerogarvity data with the objectives to determine the thickness of the sedimentary basin, establish the basement topography, density contrasts and the geological models which will give information about variation of geological structures. Four sheets of digital airborne gravity data were used for the study. Source parameter imaging (SPI), Standard Euler deconvolution and forward and inverse modeling techniques were employed in quantitative interpretation. The Bouguer anomaly of the study area varied from -20.0 to 37.7 mGal, while the residual Bouguer anomaly varied from -19.6 to 25.7 mGal. The SPI gave depth values ranging from -539.7 to -4276.0 m for shallow and deep lying gravity anomalous bodies. The windowed Euler-3D for Bouguer gravity result revealed the depth range of 1355.5 to -1518.1 m for structural index of one; 2384.5 to -3283.2 m for structural index of two and 2426.0 to -5011 m for structural index of three. The forward and inverse modeling gave the density values for the modeled profiles 1, 2, 3, 4 and 5 as 1.820, 2.410, 0.720, 2.310 and 2.100 gcm^{-3}, respectively, with their respective depths of 3872, 4228, 4880, 3560 and 2527 m. The results from this study have shown that the depth to basement and density contrast have influence on the petroleum/hydrocarbon accumulation.

Key words: Aerogravity, basement, density contrast, sedimentary.

INTRODUCTION

The gravity survey is a non-destructive geophysical technique that measures difference in the earth's gravitational field at specific locations. It could be ground gravity survey or airborne (aero) gravity survey. In geosciences, the gravity method has been widely used in different applications involving engineering exploration, regional and large scales study of geological structures, where measurements of earth's gravitational field are used to map subsurface variations in density (Biswas and Sharma, 2016; Biswas et al., 2014a, b; Mandal et al., 2015, 2013). The anomalies in the earth's gravitational field results from lateral variations in the density of subsurface rocks and the distance from the measuring point. Factors like grain density, porosity and interstitial

fluids within materials affect density contrast. Gravity data can be used in many ways to solve different exploration problems, depending on the geologic setting and rock parameters (Ezekiel et al., 2013; Okiwelu et al., 2013; Obiora et al., 2016), the data when analyzed provide insight to elements of petroleum exploration and production (Johnson, 1998; Obiora et al., 2016). The density contrasts presented by the juxtaposition of sediments with shales make detailed gravity modeling in this region a valuable exercise. The aerogravity method has found numerous applications in engineering and environmental studies including locating voids and karst features, buried stream valleys, water table and determination of soil layer thickness. The success of the gravity method depends on the different earth materials having different bulk densities (mass) that produced variations in the measured gravitational field. The gravity method has good depth penetration compared to ground penetration radar, high frequency electromagnetic and dc-resistivity techniques and is not affected by high conductivity values of near-surface clay rich soils (Mickus, 2004).

The aerogravity data are acquired with sufficient resolution which contributes towards resource-scale projects which can be used to characterize salt domes for petroleum exploration, geothermal energy investigations, monitoring of geothermal reservoirs under exploitation, inferring location of faults, and permeable areas for hydrothermal movement (Adedapo et al., 2014; Agunleti and Salua, 2015). There is generally an ambiguity in all geophysics data interpretation, this affects all geophysical data and the ambiguities that arise from different geologic configurations producing similar observed measurements (Biswas, 2015, 2016, 2017a, b; Mbah et al., 2017; Biswas et al., 2017; Singh and Biswas, 2016; Biswas and Sharma, 2015, 2014a, b; Sharma and Biswas, 2013). According to Hospers (1965), the gravity field of Niger Delta showed negative values of low magnitude covering most parts of the Niger Delta and these low values are referred to as Niger Delta minimum. Depth to basement investigation is necessary in exploration as it gives information about where matured hydrocarbons are found. The objectives of this study were to determine the thickness of the sedimentary basin, establishing the basement topography and the geological models to give information about the variation of the geological structures.

Location and geology of the Niger Delta

The study area is located in the Niger Delta region which is found in the Gulf of Guinea (Tuttle et al., 1999); it is one of the most prolific hydrocarbon basins in the world. The towns covered in the study were Olobirin, Degema, Patani and Ahoada. Niger Delta has an area of about 300,000 km^2, sediment thickness of over 10,000 km and

sediment volume of 500,000 km^3 (Okiwelu et al., 2013). Niger Delta is located between latitudes 3°30' and 4°30'N, longitude 6°00' and 7°00'E. Niger Delta sediments are divided into three distinct units of Eocene to Recent ages that form major transgressive and regressive cycles. Marine sedimentation started to evolve in the early Tertiary times according to Doust and Omatsola (1990) and over the years it has prograded a distance of more than 250 km from the Benin and Calabar flanks to the present delta front, controlled by synsedimentary faults, folding and subsidence with sediment supply mainly from the Niger, Benue and Cross Rivers accumulating up to 12,000 m thickness in some regions (Merki, 1972; Evamy et al., 1978).

The Niger Delta generally displays three vertical lithostratigraphic subdivisions: an upper delta top facies; a middle delta front lithofacies; and a lower pro-delta lithofacies. These lithostratigraphic units correspond, respectively with the continental sands of Benin Formation (Oligocencene-Recent), the alternating sand/shale paralic of Agbada formation (Eocene-Recent) and the marine prodeltashales of Akata formation (Paleocene-Recent). The sands and sandstones of Agbada formation are the main hydrocarbon reservoirs. The shape and internal structure of the Niger Delta are also controlled by fracture zones along oceanic crust. The Niger Delta sits at the southern end of Benue trough, corresponding to a failed arm of rift triple junctions (Lehner and De Ruiter, 1977). Figure 1 is the map of Niger delta region of Nigeria showing the location and geology of the study area.

MATERIALS AND METHODS

The goal of gravity survey is to locate and describe subsurface structures from the gravity effects caused by their anomalous densities (Lowrie, 2007; Telford et al., 1990). The variations in acceleration due to earth's gravity are caused by variations in subsurface geology. The aerogravity data was acquired by Nigerian Geological Survey Agency (NGSA). The materials used for this study include four gravity sheets of Olobirin (sheet 327), Degema (sheet 328), Patani (sheet 319) and Ahoda (sheet 320). The data was then transformed to an equally spaced two dimension (2D) grid using the minimum curvature method (Briggs, 1974; Webring, 1981), which fits a minimum curvature surface to data points. This was achieved using the RANGRID GX of the Oasis Montaj™ software. The gridded data helps in producing the Bouguer gravity map. The gridded sheets were digitally merged into a composite aerogravity map which preserved the sanctity of the original maps.

The qualitative interpretation was done to map subsurface structures such as intrusives which may be responsible for the anomalies. This involves the use of grids on which the anomalous values at different stations are plotted and at which contours are drawn at suitable intervals. Then, the quantitative interpretation was done to have the estimates of depths and dimensions of sources of anomalies. The techniques adopted in this study include: source parameter imaging (SPI), Euler deconvolution, forward and inverse modeling (Biswas et al., 2017; Biswas, 2016, 2015).

The source parameter imaging is a technique using an extension of the complex analytical signal to estimate potential field depths (Thurston and Smith, 1997; Nwosu, 2014). This technique is a
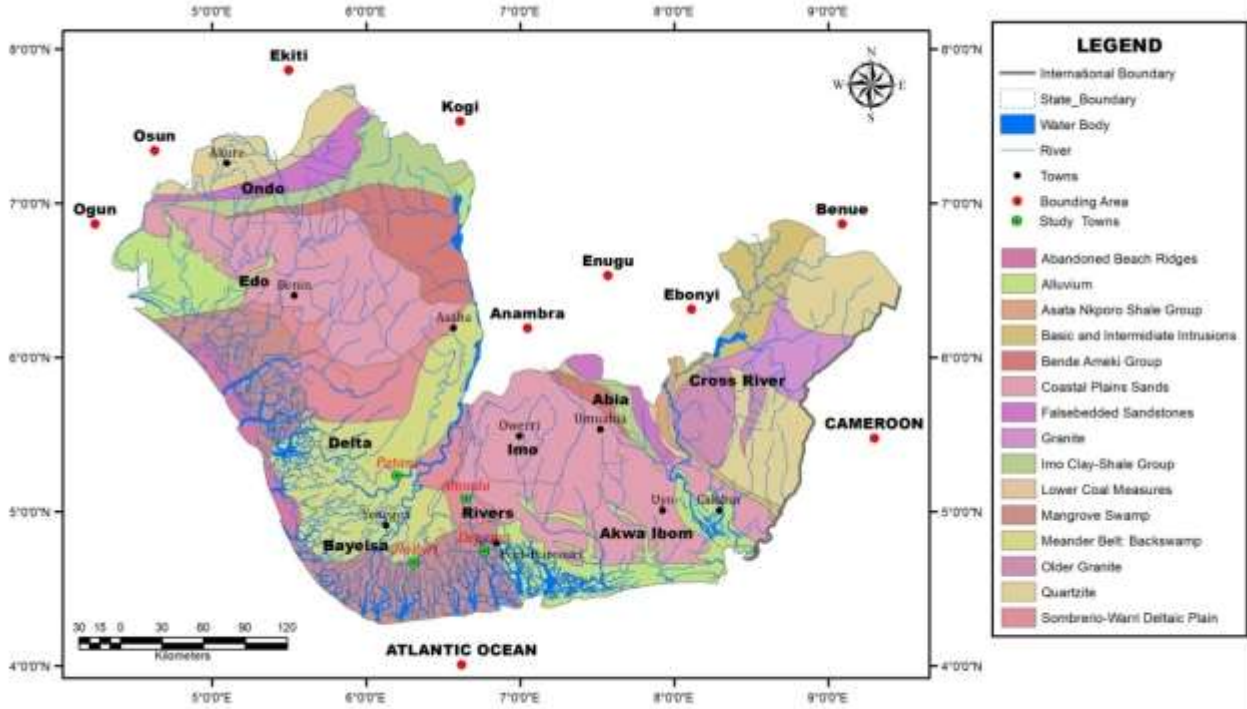
Figure 1. Map showing the location and geology of the study area.

profile or grid-based method for estimating potential source depths and for some source geometries, the dip and density contrast. The method utilizes the relationship between source depth and the local wave number (K) of the observed field, which can be calculated for any point within a grid of data via horizontal and vertical gradients (Thurston and Smith, 1997). The SPI method requires first and second order derivatives and is thus susceptible to both noise in the data and interference effects (Nwosu, 2014). The analytic signal $A_1(x, z)$ is defined by Nabighian (1972) as:

$$A_1(x,z) = \frac{\partial M(x,z)}{\partial x} - j\frac{\partial M(x,z)}{\partial z} \tag{1}$$

where M(x, z) is the magnitude of the anomalous potential field, j is the imaginary number, and z and x are Cartesian coordinates for the vertical direction and the horizontal direction perpendicular to strike, respectively. According to Nabighian (1972), the horizontal and vertical derivatives comprising the real and imaginary parts of the 2D analytical signal are related:

$$\frac{\partial M(x,z)}{\partial x} \Longleftrightarrow -j\frac{\partial M(x,z)}{\partial z} \tag{2}$$

where $\Longleftrightarrow$ denotes a Hilberts transform pair. The local wavenumber K_1 is defined by Thurston and Smith (1997) to be:

$$K_1 = \frac{\partial}{\partial x}\tan^{-1}\left[\frac{\partial M}{\partial z} / \frac{\partial M}{\partial x}\right] \tag{3}$$

Thus, the analytic signal could be defined based on second-order derivatives, $A_2(x, z)$, where

$$A_2(x,z) = \frac{\partial^2 M(x,z)}{\partial z\,\partial x} - j\frac{\partial^2 M(x,z)}{\partial^2 z} \tag{4}$$

This gives rise to a second-order local wave number K_2, where

$$K_2 = \frac{\partial}{\partial x}\tan^{-1}\left[\frac{\partial^2 M}{\partial^2 z} / \frac{\partial^2 M}{\partial z\,\partial x}\right] \tag{5}$$

The first- and second-order local wave numbers are used to determine the most appropriate model and a depth estimate independent of any assumptions about a model (Salako, 2014).

The Euler Deconvolution produces map that show the locations and corresponding depths of the geologic sources observed in a two dimensional grid. The standard Euler 3D method is based on Euler's homogeneity equation, an equation that relates the potential field and its gradient components to the location of the source, with the degree of homogeneity η which may be interpreted as a structural index, SI (Thompson, 1982). The SI is an exponential factor corresponding to the rate at which the field falls off with distance, for a source of a given geometry. The Standard 3D form of Euler's equation (Reid et al., 1990) can be defined as:

$$x\frac{\partial T}{\partial x} + y\frac{\partial T}{\partial y} + z\frac{\partial T}{\partial z} + \eta T = x_0\frac{\partial T}{\partial x} + y_0\frac{\partial T}{\partial y} + z_0\frac{\partial T}{\partial z} + \eta b \tag{6}$$

where x, y, and z are the coordinates of a measuring point; x_0, y_0, and z_0 are the coordinates of the source location whose total field is detected at x, y, and z; b is a base level; η is structural index (SI) and T is potential field. The value of the SI depends on the type of source body under investigation (Whitehead and Musselman, 2005). For example $\eta = 0$ for a horizontal contact with infinite dimensions, $\eta = 0.5$ for a vertical contact, $\eta = 1$ for top of a vertical
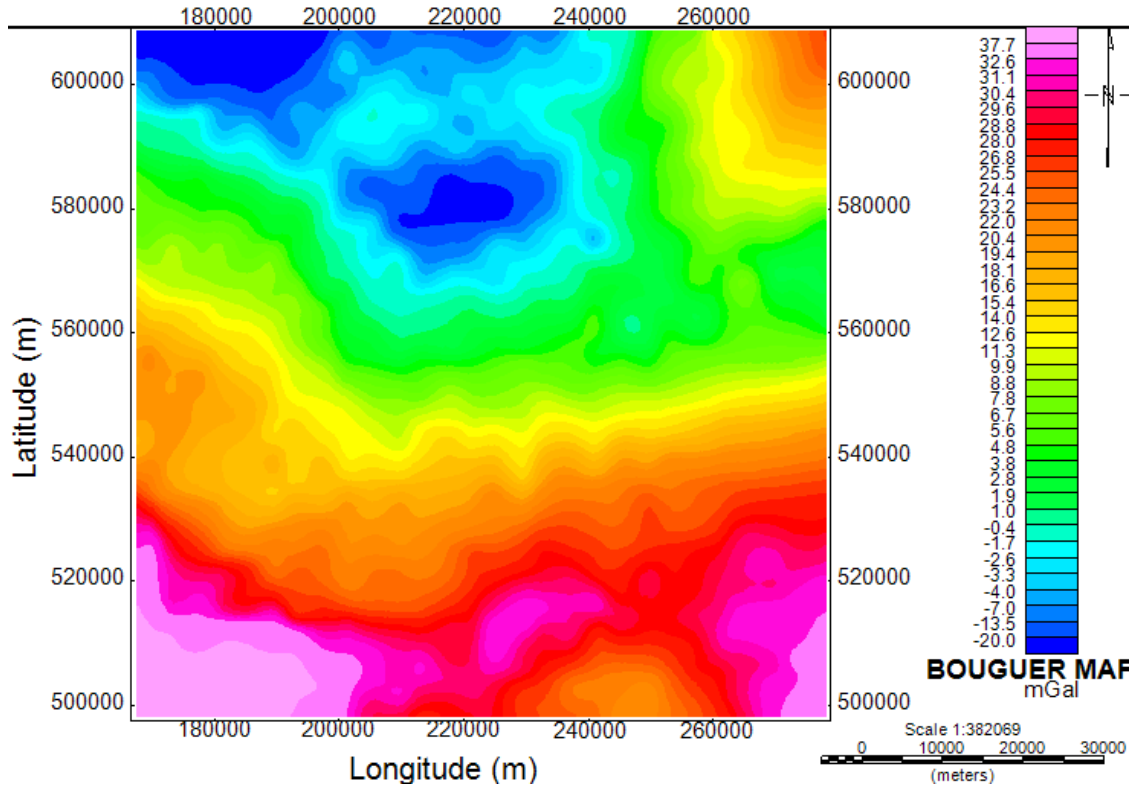
Figure 2. Bouguer gravity map of the study area.

dyke or the edge of a sill, $\eta = 2$ for the centre of a horizontal or vertical cylinder and $\eta = 3$ for the centre of a magnetic sphere or dipole (Thompson, 1982; Reid et al., 1990; Moghaddam et al., 2015).

In modeling, the PotentQ 3D tool of the Oasis montaj[TM] is used; it involves making numerical estimates of the depth and dimensions of the sources of anomalies. The forward modeling is a trial and error method; in which the shape, position and physical properties of the models are adjusted in order to obtain a good fit between the calculated field and the observed field data. The inverse modeling involves a mathematical process that automatically adjusts the model parameters so as to improve the fit between the calculated field and the observed field.

RESULTS AND DISCUSSION

The result from the interpreted data shows that Bouguer anomaly of the study area varies from -20.0 to 37.7 mGal (Figure 2). These values indicate the presence of coastal-oceanic regions where the Bouguer gravity values drops to zero as we move close to the coast (Robinson and Coruh, 1988). The regions of gravity high correspond to region with high density contrast beneath the surface and gravity low corresponds to region of low density contrast. The residual Bouguer anomaly varies from -19.6l to 25.7 mGal. The southern part of the study area has high density contrast beneath the subsurface and decreases

towards the northern part (Figure 3). The regional Bouguer anomaly varies from 11.7 to 14.4 mGal (Figure 4).

Figure 5 is the horizontal derivative computed from the residual Bouguer gravity grid using Oasis montaj[TM] software. The horizontal derivative map (Figure 5) shows more exact location for faults.

Figure 6 is the aerogravity SPI map showing the variation of depths to anomalous gravity bodies computed using the first vertical derivatives and horizontal gradient. The negative depth values depicts the depths of buried gravity bodies, which may be deep seated basement rocks or near surface intrusive. The pink colour generally indicates areas occupied by shallow gravity bodies, while the blue colour depicts areas of deep lying gravity bodies. The SPI depth result varies from -539.7 m (shallow gravity anomalous bodies) to -4276.7 m (deep lying gravity anomalous bodies). The high depths indicate thick sediment which is suitable for hydrocarbon accumulation (Wright et al., 1985, Obiora et al., 2016).

The Euler depths were estimated using vertical derivatives in three dimensions (x, y, and z), vertical derivatives enhance shallow gravity bodies. Hence, depths of shallow gravity anomalies for different structural index are displayed by Euler method. Different structural
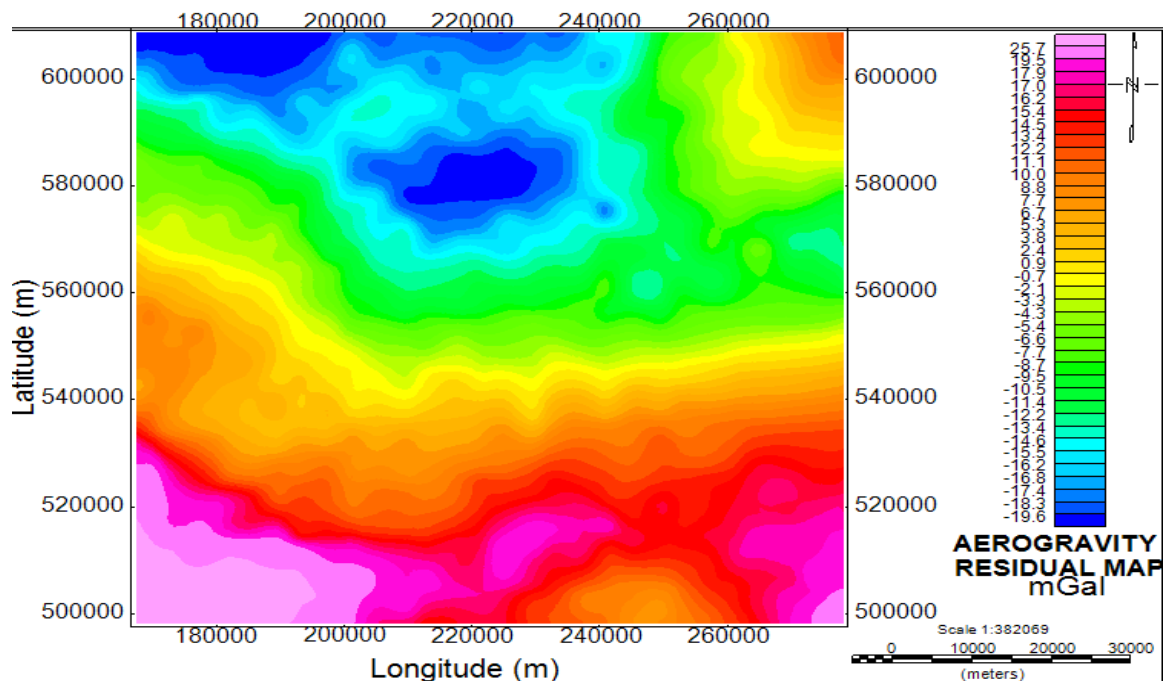
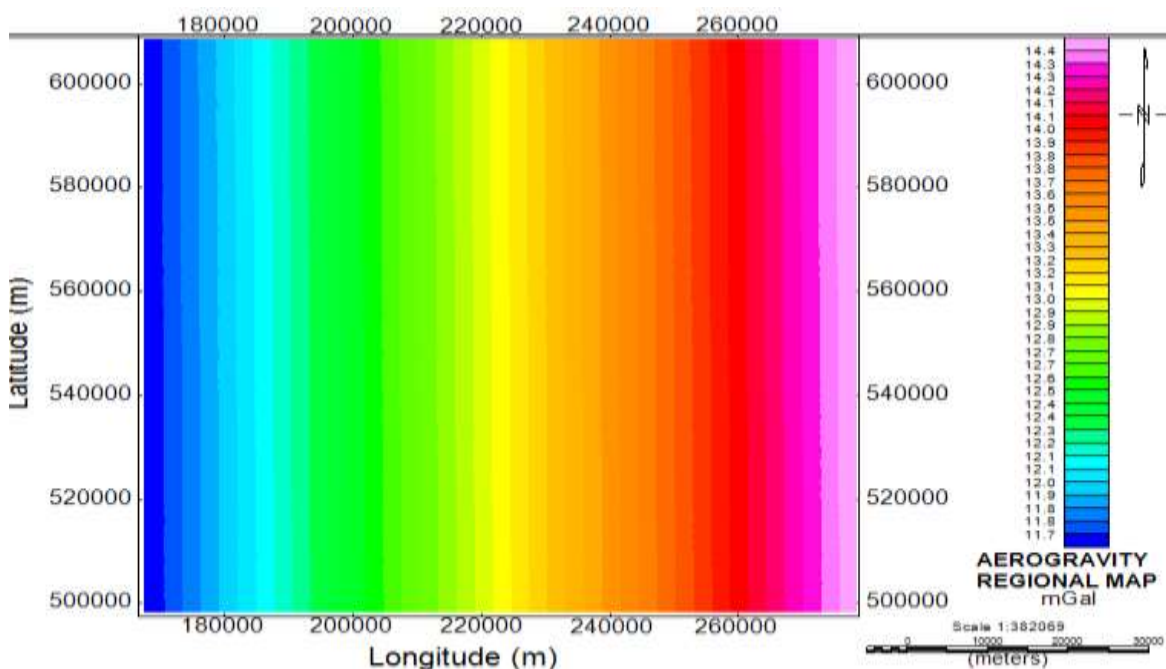**Figure 3.** Residual gravity map of the study area.

Figure 4. Regional gravity intensity map of the study area.

index numbers were tried on the data but it was found that the index number 0, 1 and 2 were the best for the data as it reflected the geological information of the area. Three Euler deconvolution maps were generated as shown in Figure 7a, b and c for the aerogravity data. The pink colour indicates shallow gravity bodies, while the blue colour indicates deep lying gravity bodies. The Euler depth result ranges from -1518.1 to 1355.5, -3283.2 to
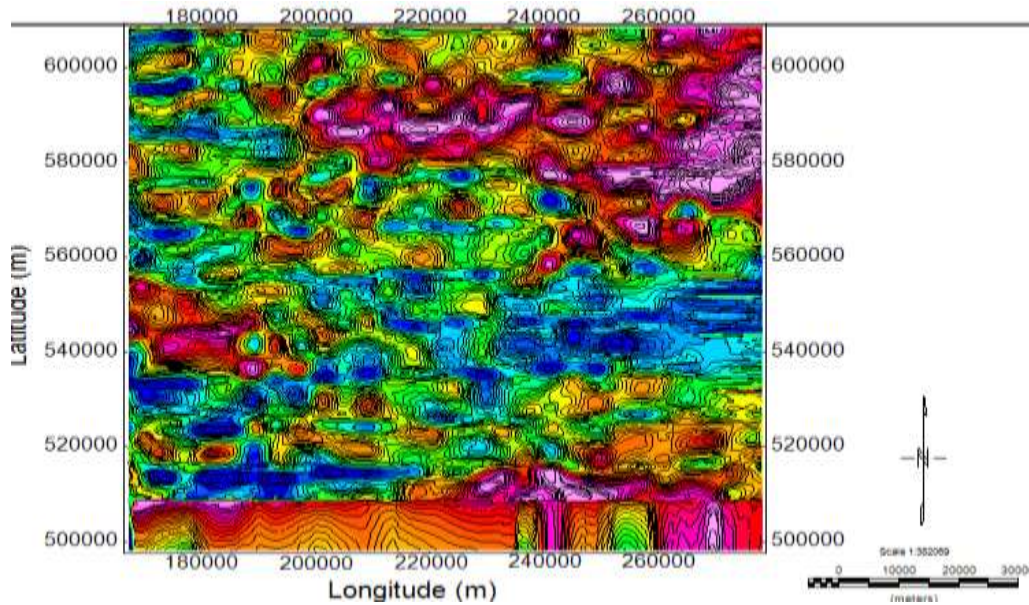
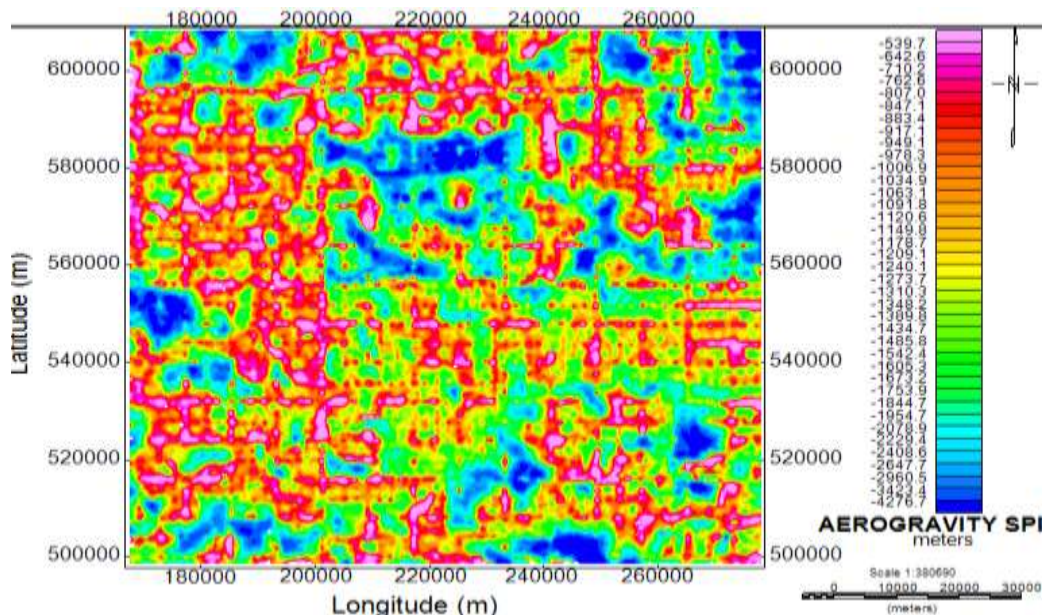**Figure 5.** Aerogravity horizontal derivative map of the study area.

Figure 6. Source parameter image (SPI) map of the study area.

2384.0 m, and -5011.4 to 2426.0 m for structural index of 0, 1, and 2, respectively. The results of Euler 3D depths are summarized in Table 1.

Five profiles were taken on the residual Bouguer grid (Figure 8) and modeled in order to show the distribution of causative bodies within the selected area. Each profile produced a degree of strike, dip and plunge where the observed values matched well with the calculated values. The blue curves represent the observed field values while the red curves represent the calculated field values. The forward modeling being a trial and error method, the shape, position and physical properties of the model were adjusted in order to obtain a good correlation between the calculated field and the observed field data. Using PotentQ 3D tool of the Oasis montaj™ software, the field of the model was calculated. The root mean square (RMS) difference between the observed and calculated field values were attempted to be minimized by the
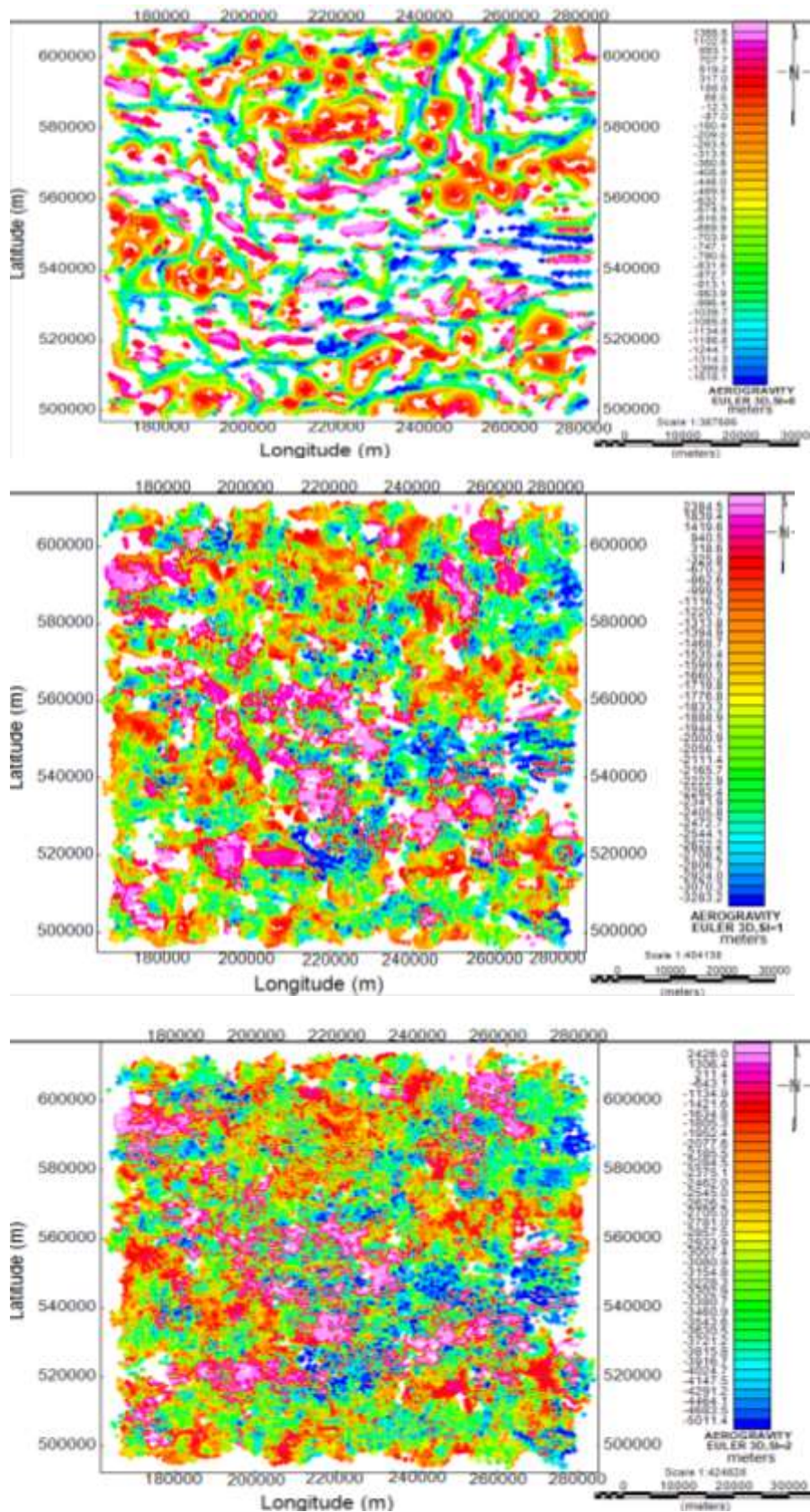
Figure 7. (a) Aerogravity Euler 3D depth map, SI=0; (b) Aerogravity Euler 3D depth map, SI=1; (c): Aerogravity Euler 3D depth map, SI=2.

Table 1. Depth estimates for Euler-3D Deconvolution.

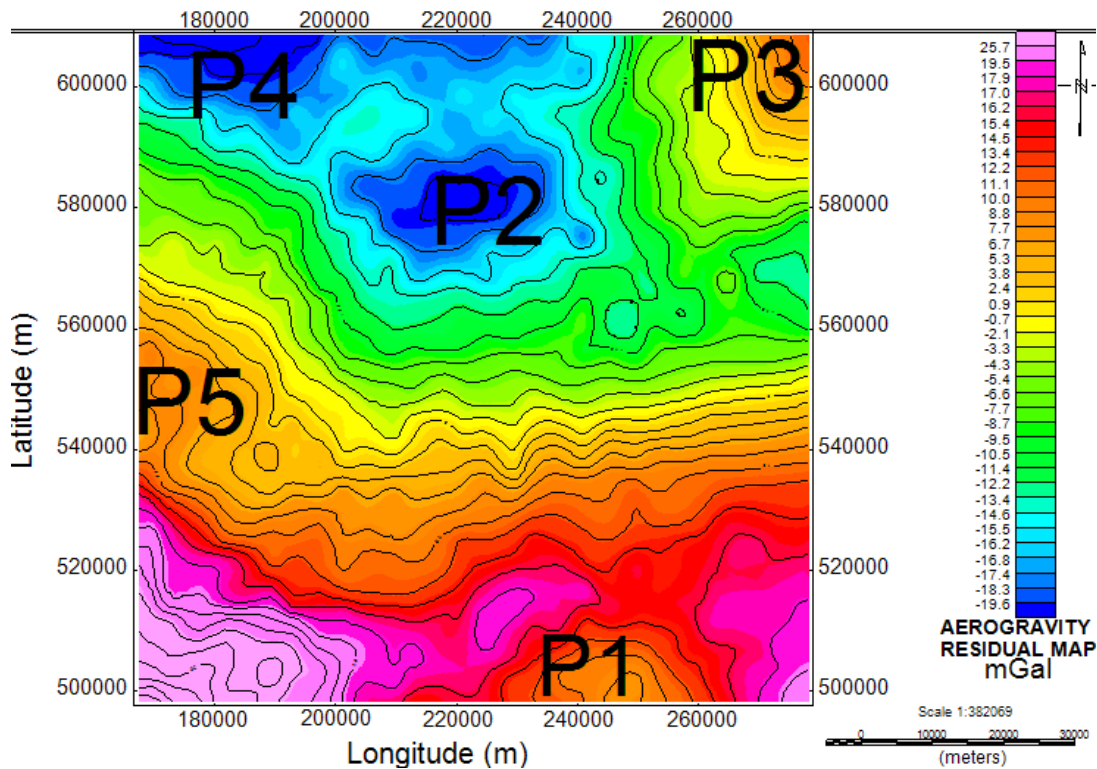| Structural index, SI	Depth ranges (m) Bouguer gravity data
0	1355.5 to -1518.1
1	2384.5 to -3283.2
2	2426.0 to -5011.4

Figure 8. Aerogravity Residual contour map.

inversion algorithm. At the end of the inversion, the RMS value was displayed. The RMS value decreased as the fit between the observed and calculated field continues to improve, until a reasonable inversion result was achieved. Less than 5% of root mean square value was set as the error margin. The modeled profiles are shown in Figure 9a to e and the results of the forward and inverse modeling are summarized in Table 2. The result from the forward and inverse modeling analysis of the aerogravity data shows that the density values obtained from the modeled profiles 1, 2, 3, 4 and 5 are 1.820, 2.410, 0.720, 2.310 and 2.100 g/cm^3, respectively, with respective depths of 3872, 4228, 4880, 3560 and 2527 m. These density values indicate the presence of minerals like petroleum, clay, gypsum, kaolinite and rock bearing minerals like shale, limestone and marble in the study area (Thompson and Oldfield, 1986; Telford et al., 1990; Hunt et al., 1995). The observed depths indicate thick sediments that confirms the feasibility for

hydrocarbon accumulation in the area.

Conclusion

Aerogravity data covering Olobirin (sheet 327), Degema (sheet 328), Patani (sheet 319) and Ahoda (sheet 320) in Niger Delta region of Nigeria were interpreted. Source parameter imaging (SPI), Euler deconvolution and forward and inverse modeling techniques were employed in quantitative interpretation with the aim of determining depth/thickness of the sedimentary basin, basement topography, density contrasts, and types of mineralization prevalent in the area.

The Bouguer anomaly of the study area varies from -20.0 to 37.7 mGal while the residual Bouguer anomaly of the study area varies from -19.6 to 25.7 mGal. These values are indicative of coastal-oceanic regions where the Bouguer gravity values drop to zero as we move
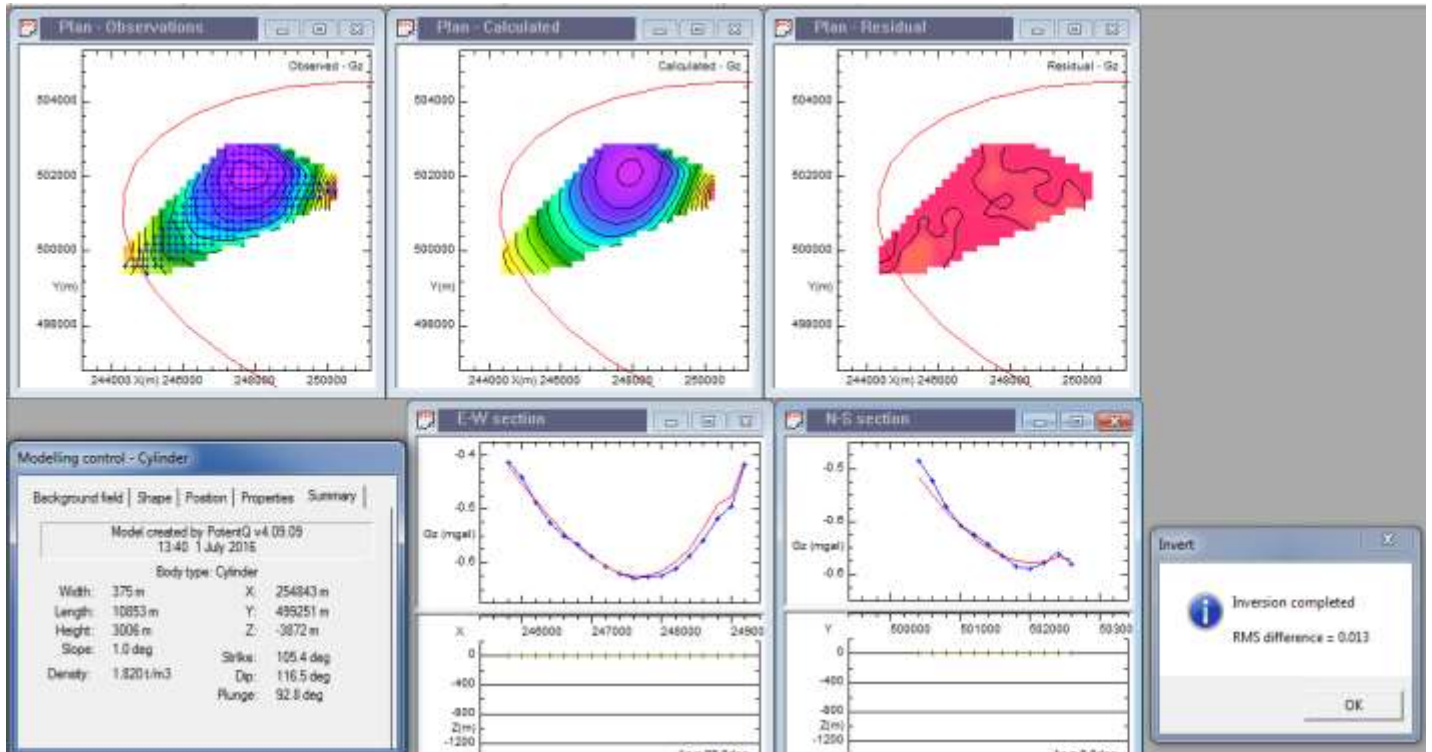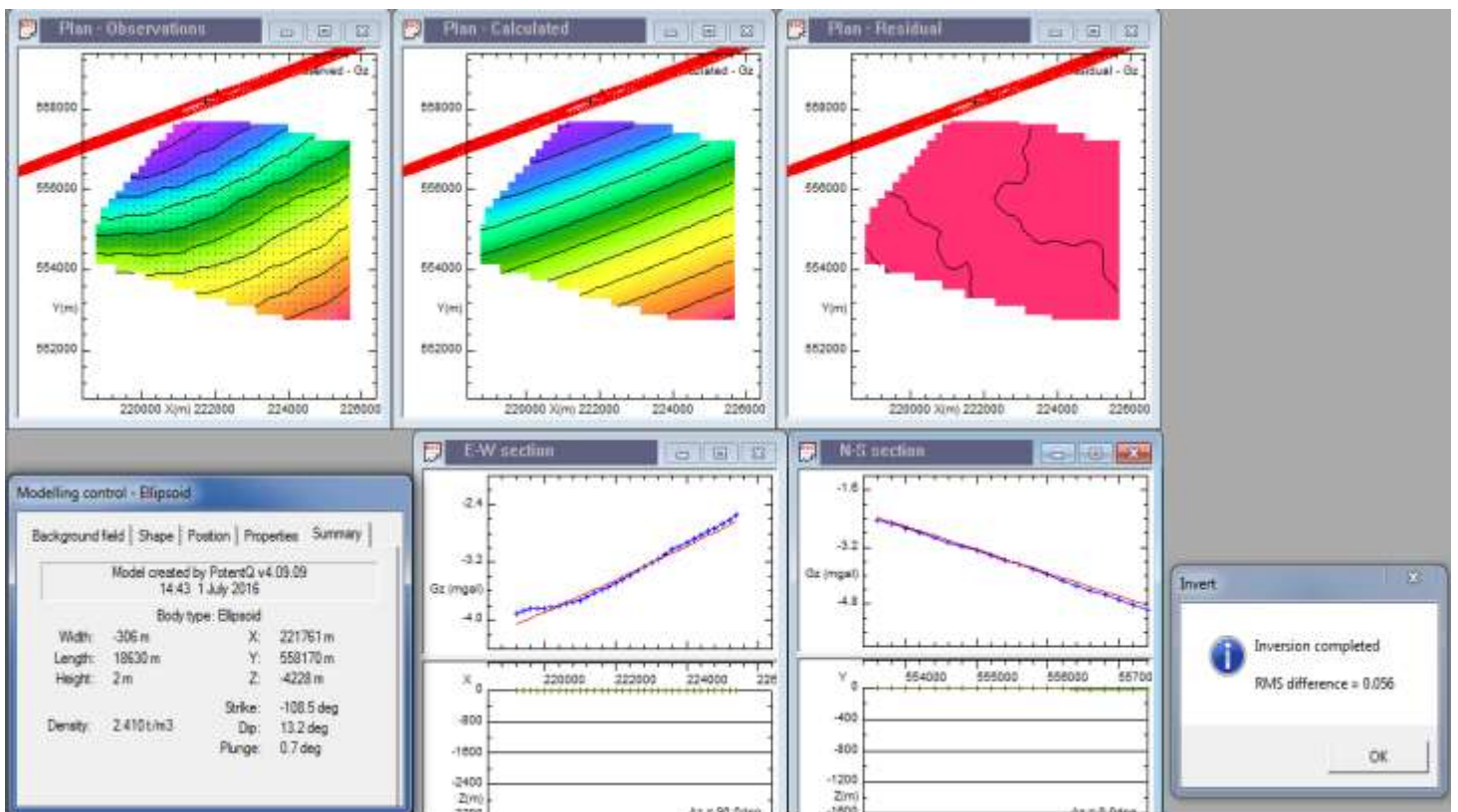
Figure 9a. Profile 1 (P1) modeled.
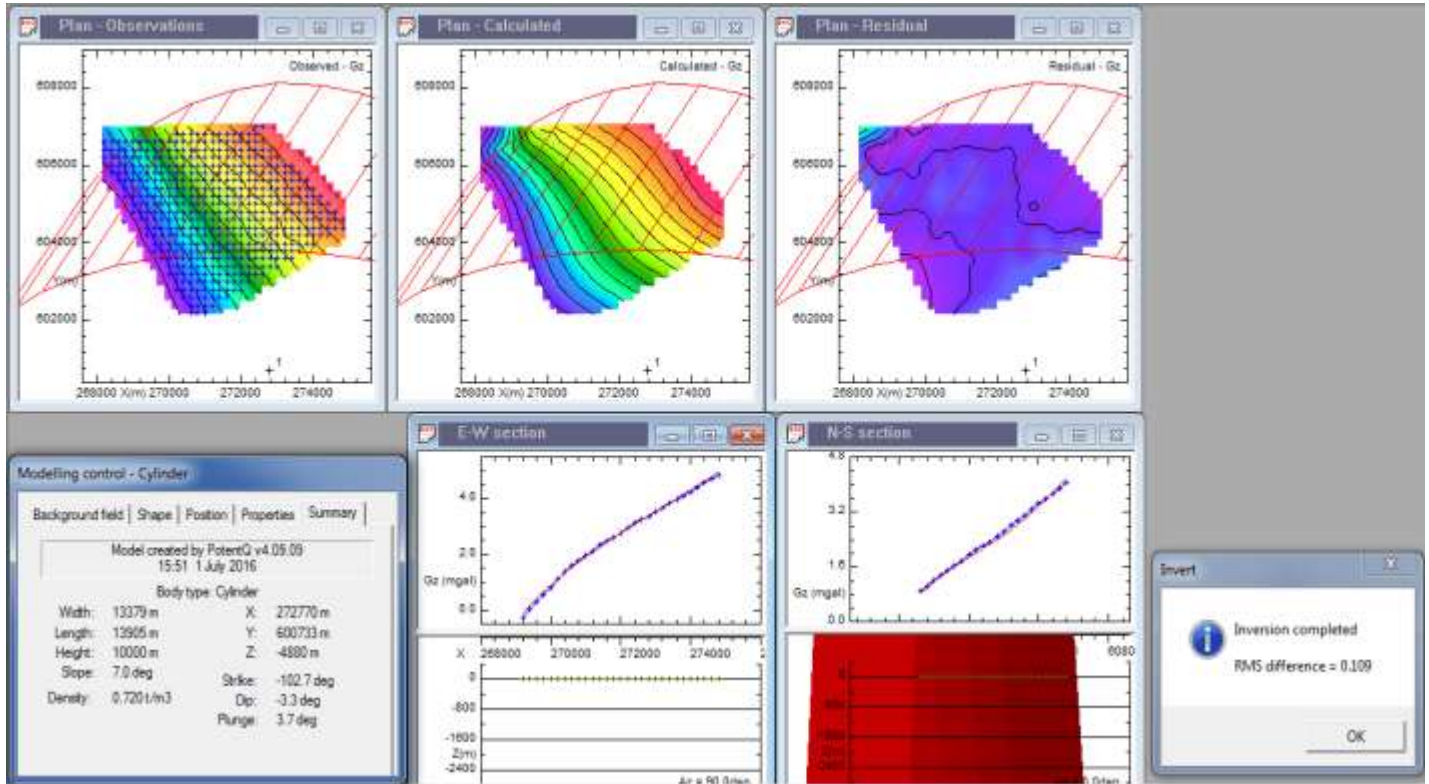

Figure 9b. Profile 2 (P2) modeled.

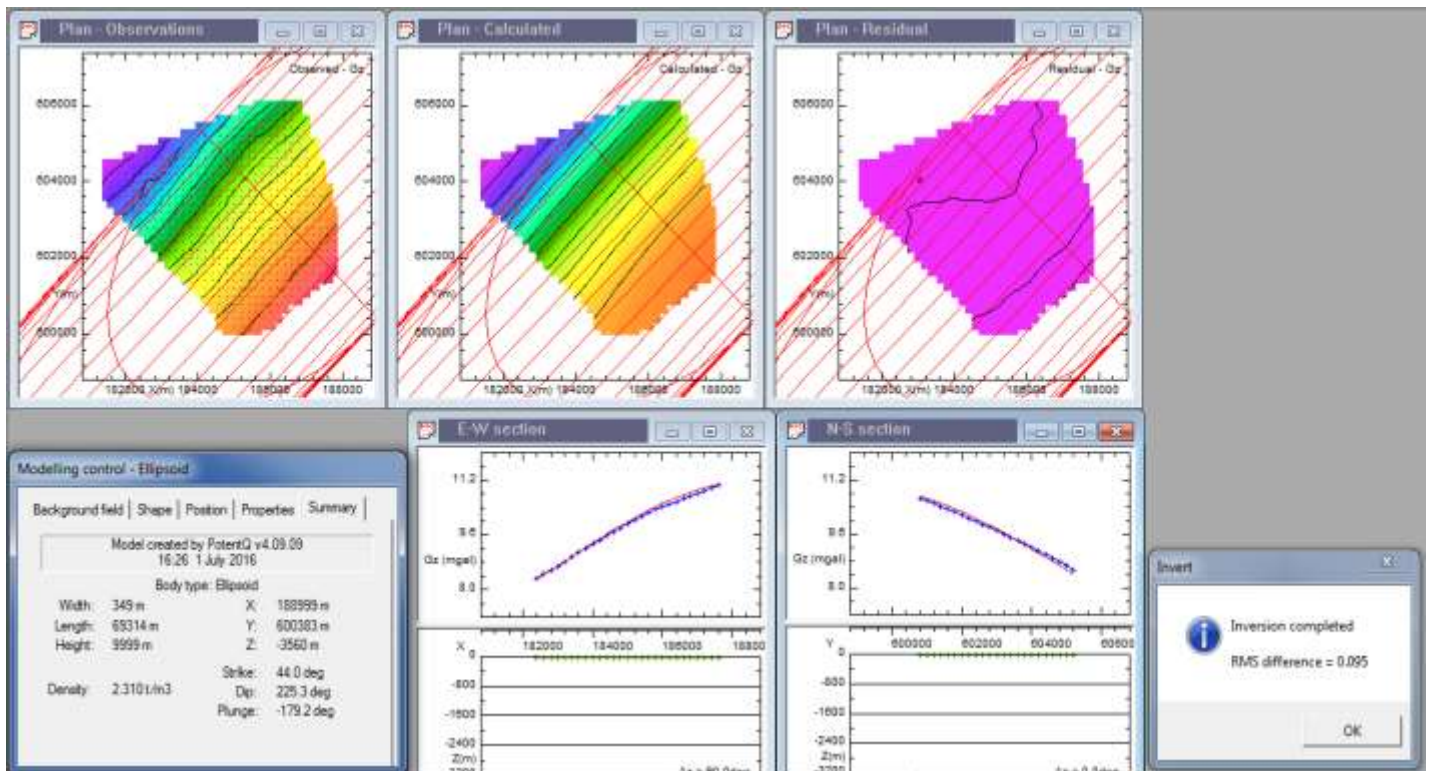**Figure 9c.** Profile 3 (P3) modeled.

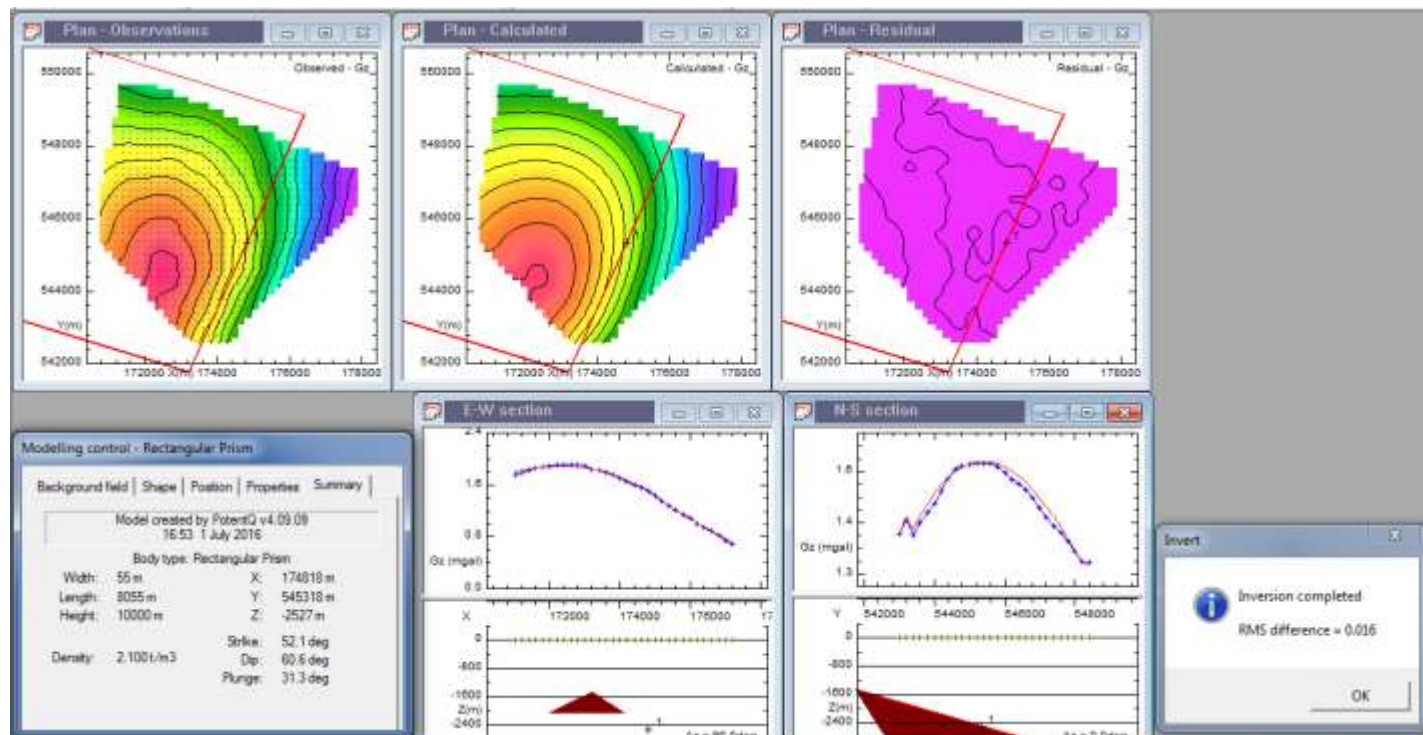**Figure 9d.** Profile 4 (P4) modeled.

Figure 9e. Profile 5 (P5) modeled.

Table 2. Summary of aerogravity forward and inverse modeling results.

Model	Model shape	X (m)	Y (m)	Depth to anomalous body (m)	Plunge (deg)	Dip (deg)	Strike (deg)	Density value (g/cm³)	Possible cause of anomaly
P6	Cylinder	254843	499251	3872	92.8	116.5	105.4	1.820	Shale
P7	Ellipsoid	221761	558170	4228	0.7	-13.2	-108.5	2.410	Gypsum
P8	Cylinder	272770	600733	4880	3.7	-3.3	-102.7	0.720	Petroleum
P9	Ellipsoid	188999	600383	3560	-179.2	225.3	44.0	2.310	Kaolinite
P10	Rectangular prism	174818	545318	2527	31.3	60.6	52.1	2.100	Limestone

close to the coast and also show the heterogeneous nature of the study area. The contour maps reveal regions with gravity high and low which correspond to regions of high and low density contrast, respectively. The source parameter image (SPI) grid indicates the different density contrast and magnetic susceptibility within the area. The SPI depth result for the aerogravity data ranges from -539.7 to -4276.7 m.

The windowed Euler-3D for the Bouguer gravity results show that for structural index of one, the depth range is between 1355.5 and -1518.1 m; for structural index of two, the depth range is between 2384.5 and -3283.2 m, while for structural index of three, it is between 2426.0 and -5011.4 m. The results from the forward and inverse modeling analysis of the aerogravity data show that the density values obtained from the modeled profiles 6, 7, 8,

9 and 10 are 1.820, 2.410, 0.720, 2.310 and 2.100 g/cm³, respectively, with respective depths of 3872, 4228, 4880, 3560 and 2527 m. The results indicated that the estimated sedimentary thickness and variation of the geological structures that makes the region is suitable for hydrocarbon and other minerals accumulation in the study area.

CONFLICT OF INTERESTS

The authors have not declared any conflict of interests.

REFERENCES

Adedapo JO, Ikpokonte AE, Kurowska E, Schoeneich K (2014). An

Estimate of Oil Window in Nigeria Niger Delta Basin from Recent Studies. Am. Int. J. Cont. Res. 4(9):114-121.

Agunleti YS, Saua SL (2015). Geochemical Studies and Exploration potential of the Oolitic-Pisolitic Ironstone deposits of Agbaja Formation Southern Bida Basin, North-central Nigeria. Int. J. Innov. Sci. Eng. Tech. 2(5):527-528.

Biswas A (2017a). A Review on Modeling, Inversion and Interpretation of Self-Potential in Mineral Exploration and Tracing Paleo-Shear Zones. Ore Geol. Rev. 91:21-56.

Biswas A (2017b). Inversion of source parameters from magnetic anomalies for mineral /ore deposits exploration using global optimization technique and analysis of uncertainty. Nat. Res. Res. DOI: 10.1007/s11053-017-9339-2.

Biswas A, Parija MP, Kumar S (2017). Global nonlinear optimization for the interpretation of source parameters from total gradient of gravity and magnetic anomalies caused by thin dyke. Ann. Geophys. 60(2):G0218, 1-17.

Biswas A, Sharma SP (2016). Integrated geophysical studies to elicit the structure associated with Uranium mineralization around South Purulia Shear Zone, India: A Review. Ore Geol. Rev. 72:1307-1326.

Biswas A (2015). Interpretation of residual gravity anomaly caused by a simple shaped body using very fast simulated annealing global optimization. Geosci. Front. 6(6):875-893.

Biswas A, Sharma SP (2015). Interpretation of self-potential anomaly over idealized body and analysis of ambiguity using very fast simulated annealing global optimization. Near Surf. Geophys. 13(2):179-195.

Biswas A, Sharma SP (2014a). Optimization of Self-Potential interpretation of 2-D inclined sheet-type structures based on Very Fast Simulated Annealing and analysis of ambiguity. J. Appl. Geophys. 105:235–247.

Biswas A, Sharma SP (2014b). Resolution of multiple sheet-type structures in self-potential measurement. J. Earth Syst. Sci. 123(4): 809–825.

Biswas A, Mandal A, Sharma SP, Mohanty WK (2014a). Delineation of subsurface structure using self-potential, gravity and resistivity surveys from South Purulia Shear Zone, India: Implication to uranium mineralization. Interpretation 2(2):T103-T110.

Biswas A, Mandal A, Sharma SP, Mohanty WK (2014b). Integrating apparent conductance in resistivity sounding to constrain 2D Gravity modeling for subsurface structure associated with uranium mineralization across South Purulia Shear Zone. Int. J. Geo. pp. 1-8.

Biswas A (2016). Interpretation of gravity and magnetic anomaly over thin sheet-type structure using very fast simulated annealing global optimization technique. Model. Earth Syst. Environ. 2(1):30.

Briggs IC (1974). Machine contouring using minimum curvature. Geophysics 39(1):39-48.

Doust H, Omatsola E (1990). Niger Delta. In *Divergent Passive Margin Basins.* JD. Edwards and PA Santogrossi (eds). American Association of Petroleum Geologists. Memoir 48:201-238.

Ezekiel JC, Onu NN, Akaolisa CZ, Opara AI (2013). Preliminary Interpretation of gravity mapping over the Njaba sub-basin of Southeastern Nigeria.An implication to petroleum potential. J. Geol. Min. Res. 5(3):75-87.

Evamy BD, Harebourne J, Kamerling P, Knaap WA, Molloy FA, Rowlands PH (1978). Hydocarbon habitat of Tertiary Niger Delta. Bull. Am. Assoc. Pet. Geol. 62(1):1-39.

Hosper J (1965). Gravity field and structure of the Niger Delta, Nigeria, West Africa. Geol. Soc. Am. Bull. 76:407-4222.

Hunt CP, Moskowitz BM, Banerjee SK (1995). Magnetic properties of rocks and minerals, in Ahrens, T.J., ed., Rock Physics and Phase Relations: A Handbook of Physical Constants. Am. Geophys. Union 3:189–204.

Johnson EAE (1998). Gravity and magnetic analyses can address various petroleum issues. Geologicapplications of Gravity and Magnetic: case Histories. In Gibson I, Millegan PS (Eds.). SEGGeophysical Reference No.8 and AAPG Studies in Geology 43:7-8. Tulsa, United States.

Lehner D, De Ruiter PAC (1977). Structural history of Atlantic margin of Africa. AAPG Bull. 61:961-981.

Lowrie W (2007). Fundamentals of Geophysics. Cambridge University Press, London.

Mandal A, Mohanty WK, Sharma SP, Biswas A, Sen J, Bhatt AK (2015). Geophysical signatures of uranium mineralization and its subsurface validation at Beldih, Purulia District, West Bengal, India: A case study. Geophys. Prospect. 63:713-726.

Mandal A, Biswas A, Mittal S, Mohanty WK, Sharma SP, Sengupta D, Sen J, Bhatt AK (2013). Geophysical anomalies associated with uranium mineralization from Beldih mine, South Purulia Shear Zone, India. J. Geol. Soc. Ind. 82(6):601-606.

Mbah D, Obiora DN, Oha AI, Terhemba BS, Ossai CO, Igwe EA (2017). Investigation of possible cause of gravity anomalies in parts of the Niger Delta basin, Nigeria. Int. J. Phys. Sci. 12(9):103-117.

Merki PI (1972). Structural Geology of the Cenozoic Niger Delta. Afr. Geol. University of Ibadan Press, pp. 251-260.

Mickus K (2004). The gravity method in engineering and environmental applications, In: Geophysics 2003: Federal Highway Administration and Florida Department of Transportation special publication.

Moghaddam MM, Sabseparvar M, Mirzaei S, Heydarian N (2015). Interpretation of Aeromagnetic Data to Locate Buried Faults in North of Zanjan Province, Iran. J. Geophys. Rem. Sens. 4:143.

Nabighian MN (1972). The analytic signal of two dimensional magnetic bodies with polygonal cross-section: Its properties and use for automated anomaly interpretation. Geophysics 37(3):507-517.

Nwosu OB (2014). Determination of Magnetic Basement Depth over Parts of Middle Benue Trough by Source Parameter Imaging (SPI) Technique Using HRAM. Int. J. Sci. Tech. Res. 3(1):262.

Obiora DN, Ossai MN, Okeke FN, Oha AI (2016). Interpretation of airborne geophysical data of Nsukka area, Southeastern Nigeria. J. Geol. Soc. Ind. 88:654-667.

Okiwelu AA, ofrey-Kulo O, Ude IA (2013). Interpretation of regional magnetic data offshore Niger Delta reveals relationship between deep basement architecture and hydrocarbon target. Earth Sci. Res. 2(1):13-32.

Reid AB, Allsop JM, Grauser H, Millet AJ, Somerton IN (1990). Magnetic interpretation in three dimensions using Euler deconvolution. Geophysics 55(1):80-91.

Robinson ES. Coruh C (1988.) Basic exploration Geophysics. New York.

Salako KA (2014). Depth to Basement Determination Using Source Parameter Imaging (SPI) of Aeromagnetic Data: An Application to Upper Benue Trough and Borno Basin, Northeast, Nigeria. Acad. Res. Int. 5(3):74-86.

Singh A, Biswas A (2016). Application of global particle swarm optimization for inversion of residual gravity anomalies over geological bodies with idealized geometries. Nat. Res. Res. 25(3):297-314.

Sharma SP, Biswas A (2013). Interpretation of self-potential anomaly over 2D inclined structure using very fast simulated annealing global optimization–An insight about ambiguity. Geophysics 78(3):WB3–15.

Telford WM, Geldart LP, Sheeriff RE (1990). Applied geophysics (2nd edition). Cambridge University press, Cambridge.

Thompson DT (1982). A new technique for making computer-assisted depth estimates from magnetic data. Geophysics 47(1):31-37.

Thompson R, Oldfield F (1986). Environmental Magnetism: London, Allen and Unwin, 227.

Thurston JB, Smith RS (1997). Automatic conversion of magnetic data to depth, dip, and susceptibility contrast using the SPI[TM] method. Geophysics 62(3):807-813.

Tuttle MLW, Charpentier RR, Brownfield ME (1999). The Niger Delta petroleum system: Niger Delta province, Nigeria, Cameroun and Equatorial Guinea, Africa, U. S. Geological Survey Open-fileReport-99-50-H, 31P.

Webring M (1981). MINC: a gridding program based on minimum curvature. *U.S. Geological Survey* 81-1224:43.

Whitehead N, Musselman C (2005). Montaj[TM]Grav/Mag interpretation: Processing, analysis and visualization system for 3D inversion of potential field data for Oasis montaj v6.1. Geosoft Inc. ON, Canada.

Wright JB, Hastings D, Jones WB, Williams HR (1985.) Geology and Mineral Resources of West Africa. George Allen and Unwind publ. London.